



## Mercury removal from drinking water by single iron and binary iron-manganese oxyhydroxides

Evgenios Kokkinos<sup>a</sup>, Konstantinos Simeonidis<sup>a</sup>, Anastasios Zouboulis<sup>b</sup>,  
Manassis Mitrakas<sup>a,\*</sup>

<sup>a</sup>Department of Chemical Engineering, Aristotle University of Thessaloniki, Thessaloniki 54124, Greece, emails: [kokkinosevgenios@yahoo.gr](mailto:kokkinosevgenios@yahoo.gr) (E. Kokkinos), [ksime@physics.auth.gr](mailto:ksime@physics.auth.gr) (K. Simeonidis), [manasis@eng.auth.gr](mailto:manasis@eng.auth.gr) (M. Mitrakas)

<sup>b</sup>Department of Chemistry, Aristotle University of Thessaloniki, Thessaloniki, Greece, email: [zoubouli@chem.auth.gr](mailto:zoubouli@chem.auth.gr)

Received 6 August 2013; Accepted 26 February 2014

### ABSTRACT

In this study, single iron oxyhydroxides (FeOOH) and binary iron/manganese (FeMnOOH) oxyhydroxides were used to serve as potential mercury adsorbents. The selection of the optimum adsorbent and the corresponding conditions of the synthesis was based not only on its maximum Hg(II) adsorption capacity but also on its ability to achieve the mercury health regulation limit for drinking water in National Sanitation Foundation challenge water matrix. The experimental results revealed improved adsorption capacity for Hg by the FeMnOOH compared to FeOOH. In addition, the synthesis parameters of FeMnOOH, pH, and redox showed a significant influence on Hg removal efficiency. High redox values and mild alkaline pH improve mercury removal capacity of binary ferric manganese oxyhydroxides.

*Keywords:* Mercury removal; Ferric-manganese oxyhydroxides; Adsorption; Kinetic; Surface charge

### 1. Introduction

The knowledge of the scientific community on the four interrelated parts of mercury's biogeochemical cycle (air, land, water, and living) has increased significantly over the last decade. It is estimated that the total annual global input to the atmosphere, which is the main route of Hg entry into the environment, exceeds  $5 \times 10^3$  tons [1]. Both natural and anthropogenic processes may be the sources of Hg release. Mercury is introduced in the natural environment as a

result of the friction of minerals, rocks, and soil from exposure to air and water (erosion) and the volcanic activity. However, anthropogenic emissions are still responsible for a significant proportion of global Hg in the environment although they follow a decreasing trend in recent decades. Production of chlorine and caustic soda, paper manufacturing, mining, industrial paints, laboratory, clinical and dental waste, pesticides, fossil fuels, cement production [2], industrial incinerators, waste treatment plants [3] are some cases of this category. Unlike natural sources, human activities can emit different types of mercury

\*Corresponding author.

*Presented at the 1st EWaS-MED International Conference on Improving Efficiency of Water Systems in a Changing Natural and Financial Environment, 11–13 April 2013, Thessaloniki, Greece*

including gaseous elemental mercury, particulate mercury, and reactive gaseous mercury [1].

Elemental, inorganic, and organic forms of Hg are the major forms met in the environment being highly toxic to humans, as they accumulate in the water effectively, thus passing into the food chain [4]. In natural waters, mercury may exist in three oxidation states namely  $\text{Hg}^0$  (elemental),  $\text{Hg}^+$  and  $\text{Hg}^{2+}$  with the last specie being the dominant. Its appearance and allocation depends on the pH, the redox potential, the nature, and the concentration of anions which form stable bonds with mercury [5]. Ionic  $\text{Hg}^{2+}$  are easily associated to anions, such as,  $\text{HgX}_2$ ,  $\text{HgX}^{3-}$  and  $\text{HgX}_4^{2-}$ , where  $X = \text{OH}^-$ ,  $\text{Cl}^-$ , and  $\text{Br}^-$  [6]. But mercury can also form stable structures with a plurality of organic compounds and preferably with S-structures like cysteines, amino- and hydroxyl-carboxylic acids by strong covalent bonds [5].

In order to face the problem of Hg presence in drinking water, a number of treatment processes has been applied including coagulation/filtration, ion exchange and sorption onto biomaterials, activated carbon, and inorganic adsorbents. Coagulation/filtration efficiently removes mercury to sub-ppb level fulfilling the maximum contaminant level (MCL) of  $1 \mu\text{g/L}$  [7–9]. However, the handling of produced sludge, along with the management of dewatered product, are considered as the main disadvantages of this process, contributing significantly to the increase of the respective treatment cost. On the other side, ion exchange is an attractive method for metals capture including Hg but its applications is generally focused in removal/recovery of relatively high (metals) concentrations from wastes rather than trace mercury removal from potable water [10]. The high capital cost along with the handling of the regeneration solution with high mercury concentration is the major drawbacks of this process. Considering biosorption, a wide assortment of biomaterials was studied for mercury uptake [11–13]. However, the results usually focus on high initial mercury concentrations commonly encountered in wastewaters, which in turn resulted in equilibrium mercury concentrations much higher than the MCL for drinking water. Even when low initial concentrations were used, the removal capacities achieved at equilibrium concentrations equal to the MCL were found in the range of a few ng Hg/mg that is of no practical importance [14]. In addition, biomaterials present the significant drawback of enriching treated water with organic matter, which is not always consistent with drinking water regulations.

Adsorption is a process that offers many advantages including simple and stable operation, easy handling of waste, absence of added reagents, compact

facilities, and generally lower labor cost. A large number of natural materials and synthetic inorganic adsorbents have been reported to remove Hg efficiently, but only under acidic conditions and/or high equilibrium concentrations oriented to wastewater treatment [15–21]. In particular, the most studied class of adsorbents, activated carbons, appears effective in acidic environment and high Hg concentrations, but generally do not meet drinking water MCL [22,23]. Similarly, ETS-4 titanosilicate [16],  $\text{MnO}_2$  nanowhiskers [17] and hydrous manganese and tin oxides [18] showed good mercury removal capacity, at pH values below 5, which results in the deterioration of treated water quality. Modified magnetic iron oxide nanoparticles [19,20] and hydrogen metal sulfide [21] achieved residual concentrations that meet MCL, at slightly acidic solution pH.

Iron oxyhydroxides ( $\text{FeOOH}$ ) are widely practiced for the efficient removal of various heavy metals from drinking water [24–26]. Such materials are already produced in industrial scale with low cost and grain sizes suitable for adsorption bed implementation. However, to the best of our knowledge, although mercury sorption on iron oxyhydroxides has been modeled [27,28], their adsorption efficiency for Hg has not been extensively studied, especially at the low concentrations usually met in potable water. Based on the previous work concerning the optimization of single Fe and binary Fe/Mn oxyhydroxides for drinking water treatment [29,30], the aim of this study was to investigate the potential of using these materials for efficient mercury adsorption. Specifically, the role of synthesis parameters on the determination of surface charge area and density, that mostly defines Hg adsorption capacity, was thoroughly examined. Various oxyhydroxides, prepared under different pH and redox conditions, were tested in a preliminary step on tuning the synthesis parameter for optimum mercury's removal.

## 2. Materials and methods

### 2.1. Adsorbents

The studied single iron ( $\text{FeOOH}$ ) and binary iron-manganese ( $\text{FeMnOOH}$ ) oxyhydroxides were produced by oxidation/precipitation of  $\text{FeSO}_4 \cdot \text{H}_2\text{O}$  using  $\text{H}_2\text{O}_2$  and  $\text{KMnO}_4$ , respectively, in a two-step continuous flow process. The detailed process and the corresponding physicochemical and structural characteristics are described in our previous works [29,30]. In brief, the synthesis was performed at pH values ranging between 4 and 9 rigidly controlled by NaOH addition, while the redox potential was adjusted to

reach (i) the maximum value that could be achieved at the specific pH by regulating the  $\text{H}_2\text{O}_2$  inflow in the case of  $\text{FeOOH}$  or (ii) the value ensuring a Mn valence close to +4 by adding  $\text{KMnO}_4$ , which also served as a manganese source, in the case of  $\text{FeMnOOH}$ . In order to study the effect of manganese valence, various  $\text{FeMnOOH}$  samples were synthesized at pH 6 and redox potential range between 285 and 780 mV. For comparison, the two widely practiced and commercially available iron oxyhydroxides GFH and BAYOXIDE were also tested.

The isoelectric point (IEP) in a water dispersion of oxyhydroxide solid was determined by the curve of zeta-potential at  $20 \pm 1^\circ\text{C}$ . The preparation of the samples involved the suspension of 50 mg fine oxyhydroxide powder into 1 L of electrolyte solution (0.01 M  $\text{NaNO}_3$ ). Quantities of 100 mL were equilibrated at different pH values (3–10) for 60 min under stirring by adding either  $\text{HNO}_3$  or  $\text{NaOH}$ . Then, the electrophoretic velocity of at least 100 particles was determined through a digital camera using a Rank Brothers Micro-electrophoresis Apparatus Mk II device and the  $\zeta$ -potential value was calculated.

The surface charge density of the adsorbents, as well as the point of zero charge (PZC), was found by the potentiometric mass titration method [31]. Dispersions of 10 g/L in  $10^{-3}$ – $10^{-1}$   $\text{NaNO}_3$  were adjusted to the pH 11 by adding 0.1 M  $\text{NaOH}$ . Then, the dispersions were titrated by adding stepwise small quantities of a 0.1 N  $\text{HNO}_3$  solution and recording equilibrium pH till it reached 3. Plotting of surface charge density for the three ionic strengths, which is proportional to the difference of acid volume used to bring about the same pH in the dispersion and a blank titration, indicates the PZC as the point of intersection. The total anion-exchange yield, which is related to the maximum number of exchangeable  $\text{OH}^-$ , was calculated after a similar titration of dispersions in 0.01  $\text{NaNO}_3$  till the PZC and discard of the solid. More specifically, the pH of the dispersion was adjusted to 3 by adding 0.1 M  $\text{HCl}$ . Then, the oxyhydroxide's solids were discarded and the solution was back-titrated till the PZC with 0.1 M  $\text{NaOH}$  to calculate the total cation exchange yield, which is related to the maximum number of exchangeable  $\text{H}^+$  [32]. The specific surface area (SSA) of the adsorbent samples was estimated by nitrogen gas adsorption at 77 K using a micropore surface area analyzer according to Brunauer–Emmett–Teller model.

## 2.2. Reagents

A 1,000 mg/L  $\text{Hg(II)}$  stock solution was prepared by dissolving 1.080 g of reagent grade  $\text{HgO}$  in a

volume of (1:1)  $\text{HCl}$ , and diluting to 1 L with distilled water. Working standard solutions were prepared by proper dilution of the stock solution in distilled water or National Sanitation Foundation (NSF) standard water in order to study the actual adsorption capacity in the presence and concentrations of common ions that usually met in natural waters. The NSF water was prepared by dilution: 252 mg  $\text{NaHCO}_3$ , 12.14 mg  $\text{NaNO}_3$ , 0.178 mg  $\text{NaH}_2\text{PO}_4 \cdot \text{H}_2\text{O}$ , 2.21 mg  $\text{NaF}$ , 70.6 mg  $\text{NaSiO}_3 \cdot 5\text{H}_2\text{O}$ , 147 mg  $\text{CaCl}_2 \cdot 2\text{H}_2\text{O}$ , and 128.3 mg  $\text{MgSO}_4 \cdot 7\text{H}_2\text{O}$  in 1 L of distilled water. Prior to adsorption experiments the pH was adjusted to the target value by adding either  $\text{NaOH}$  or  $\text{HNO}_3$ .

## 2.3. Adsorption evaluation

Batch experiments of mercury uptake were carried by placing 10–25 mg fine powder of samples (<63  $\mu\text{m}$ ) in 300 mL conical flasks and equilibrating with 200 mL of aqueous  $\text{Hg(II)}$  solution. The pH was adjusted to 7 and after shaking the flasks for 24 h, the suspension was filtered through a 0.45  $\mu\text{m}$  pore size membrane filter. Initial (100–250  $\mu\text{g/L}$ ) and residual mercury concentrations were determined by a Bacharach cold vapor mercury analyzer system (Coleman-Model 50B). Iron and manganese concentration in treated water was determined by flame atomic absorption spectrophotometry using a Perkin Elmer AAnalyst 800 instrument.

## 3. Results and discussion

### 3.1. Influence of adsorption pH

The effect of solution pH on mercury removal was examined for the binary  $\text{Fe/Mn}$  oxyhydroxide synthesized at pH 6. Fig. 1 illustrates the adsorption efficiency dependence on treated water's pH according to the corresponding residual  $\text{Hg}$  concentration. Importantly, the optimum range of operation is situated at the pH values commonly encountered in drinking water (pH 6–9) where efficiency is almost constant and reaches the sub-ppb level. Adsorption capacity sharply diminishes at equilibrium pH values below 6 and smoothly reduces at pH values higher than 10. These findings are consistent with those of Lisha et al. [17] and can be explained by considering mercury's speciation and the observed surface charge of oxyhydroxides. More specifically,  $\text{Hg(OH)}_2$  is the dominant form at the pH range 4–14 but the proportions of  $\text{Hg(OH)}^+$  and  $\text{Hg(OH)}^{3-}$  gradually increase below 7 and above 11, respectively. At solution pH values lower than 4,  $\text{Hg}^{2+}/\text{Hg(H}_2\text{O)}_6^{2+}$  are the main ions in water [33]. The effective surface charge of oxyhydroxides is

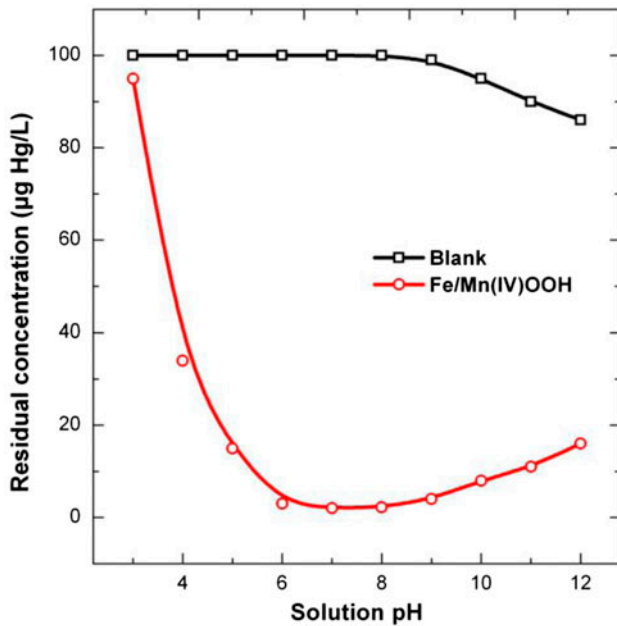


Fig. 1. Influence of solution pH on Hg uptake by the FeMnOOH prepared at pH 6 and redox 780 mV. Initial concentration 100 µg Hg/L in distilled water and adsorbent dose 100 mg/L.

defined by synthesis pH and can be described by the IEP of each sample (Fig. 2). As concluded, when the preparation pH is below 5.5, the oxyhydroxide appears positively charged at solution pH 7 while it

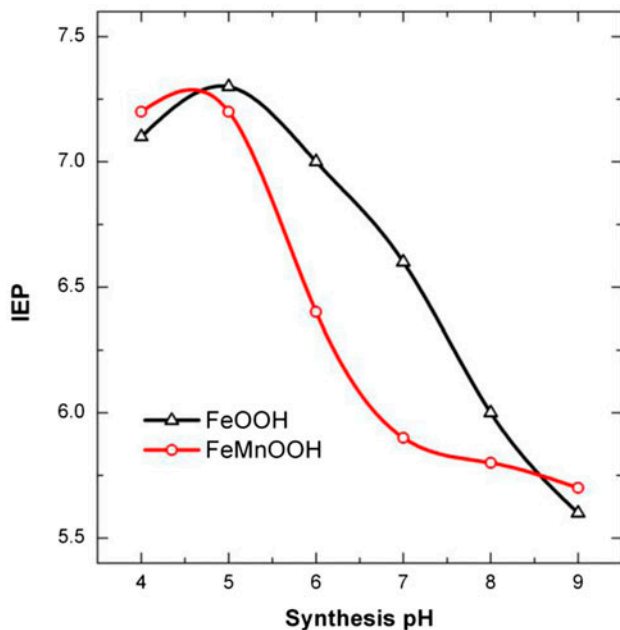


Fig. 2. IEP of oxyhydroxides used in this study.

turns negative when synthesized at pH above 6. Therefore, in neutral pH, the reaction of the dominant  $\text{Hg}(\text{OH})_2$  and hydrolyzed  $\text{Hg}(\text{OH})^+$  species with the weakly negative FeMnOOH surface, results in the formation of  $\equiv\text{M}-\text{OH}-\text{Hg}$  bonds [34].

In contrast, at solution pH lower than 5, oxyhydroxide's surface becomes strongly positive (Fig. 2) and repulses the  $\text{Hg}^{2+}/\text{Hg}(\text{H}_2\text{O})_6^{2+}$  cations resulting in low mercury uptake. Despite the contribution of spontaneous Hg precipitation at pH values above 9, depicted by the mercury's concentration drop in blank samples, the Hg uptake at pH higher than 10 decreases, as it was also reported by other studies [19,33,34]. Such behavior is probably attributed to the increase in hydroxyls ( $\text{OH}^-$ ) concentration favoring the formation of  $\text{Hg}(\text{OH})_3^-$  oxyanions [33], which are repulsed by the highly negatively charged oxyhydroxides' surface. In addition, the results of Fig. 1 can also be utilized for developing a regeneration procedure. By treating spent adsorbents with a mild acidic solution (pH 4) leaching of adsorbed mercury is expected, resulting in turn in adsorbent's refreshing. Mercury could be then easily recovered from the regeneration solution as mercury sulfide ( $K_{\text{sp}} = 1 \times 10^{-50}$ ).

### 3.2. Adsorption kinetics

Kinetic data for mercury uptake by the FeMnOOH sample prepared at synthesis pH 4 and redox 800 mV were obtained both in distilled and NSF water equilibrated at pH 7 (Fig. 3), in order to illustrate the influence of ions commonly encountered in natural waters to mercury adsorption kinetics and capacity. The experimental results for mercury adsorption in distilled as well as in NSF water matrix showed that the mercury uptake proceeds at rapid rate during the first 1 h, with more than 50% being removed within 5 min and more than 85% within 1 h, and then considerably slow down, reaching equilibrium at about 6 h. The kinetic data for mercury were best fitted to a pseudo-second-order model:

$$\frac{t}{Q_t} = \frac{1}{k_2 Q_e^2} + \frac{t}{Q_e} \quad (1)$$

where  $k_2$  is the rate constant for pseudo-second-order rate kinetics ( $\text{mg } \mu\text{g}^{-1} \text{ min}^{-1}$ ),  $Q_t$  and  $Q_e$  the amount of mercury removed ( $\mu\text{g Hg}/\text{mg FeMnOOH}$ ) at time  $t$  and at equilibrium, respectively. The pseudo-second-order function has been widely applied to describe the removal of contaminants from aqueous solutions assuming that a chemisorption process involves

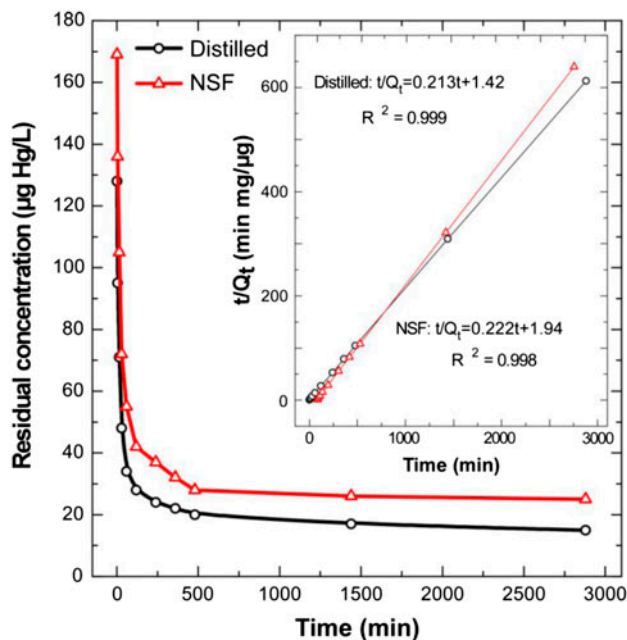


Fig. 3. Kinetic data for mercury removal and fitting in pseudo-second-order model (inset). Initial concentration  $250 \mu\text{g Hg/L}$  in distilled water at pH 7, adsorbent FeMnOOH prepared at pH 6, redox 780 mV, and dose 50 mg/L.

covalent forces and ion exchange [35]. By plotting  $t/Q_t$  vs. time the values of  $Q_e = 4.7 \mu\text{g/mg}$  and  $k_2 = 0.032 \text{ mg } \mu\text{g min}^{-1}$  were calculated for distilled water from the slope and intercept, respectively (Fig. 3 inset). The corresponding values calculated for NSF water was  $Q_e = 4.5 \mu\text{g/mg}$  and  $k_2 = 0.026 \text{ mg } \mu\text{g min}^{-1}$ , which indicate that common ions of water both depress adsorption kinetic of mercury by almost 20% and diminish the adsorption capacity close to 5%. This dictates the necessity of carrying out adsorption tests in natural-like water in order to get reliable and realistic information. In addition, to be on the safe side, a 24 h contact time was established in mercury adsorption experiments.

### 3.3. Influence of synthesis pH and redox

In order to evaluate the studied samples according to their Hg removal efficiency and understand the effect of synthesis pH and redox on adsorption mechanism, batch adsorption tests were performed in NSF water equilibrated at pH 7 (Fig. 4). In general, synthesis pH does not seriously influence the adsorption of Hg by FeOOH samples whereas Fe/Mn oxyhydroxides appear more efficient in the whole studied pH range and improve their properties at pH values

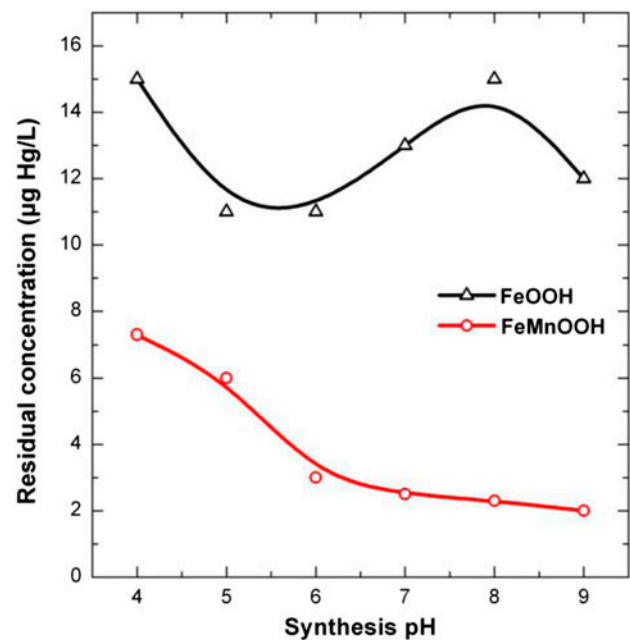


Fig. 4. Influence of synthesis pH of Fe(OOH) and binary Fe/Mn(OOH) on Hg removal efficiency. Initial concentration  $100 \mu\text{g Hg/L}$  in NSF water, adsorbent dose 100 mg/L, pH 7.

above 6. To explain the different behavior of the samples under similar conditions of application, it was attempted to correlate the results with the net surface charge density that describes the actual charge at the materials surface instead of the IEP measurements which represent the observed electrokinetic charge density.

Due to the excess of  $\text{H}^+$  in the reaction solution, oxyhydroxides' surfaces become highly positively charged when prepared at acidic pH, while the negative charge density gradually increases as pH moves to alkaline range due to  $\text{OH}^-$  dominance, respectively (Fig. 5). However, in the case of the FeOOH samples, positive charge density ( $\text{mM } [\text{OH}^-]/\text{g}$ ) remains significantly higher than the negative one ( $\text{mM } [\text{H}^+]/\text{g}$ ), although they tend to become equal as synthesis pH increases (Fig. 5(a)).

Therefore, the fact that residual Hg concentration for the FeOOH samples meets limitations to decrease below a constant value ( $13 \mu\text{g/L}$ ), is attributed to the presence of intense net positive charge, which repulses the positively charged species of mercury. Although the same pattern is followed in charge density values of FeMnOOH samples, their improved efficiency may be related to the higher values of negative charge density curve most probably caused by the charge destabilization during incorporation of tetravalent

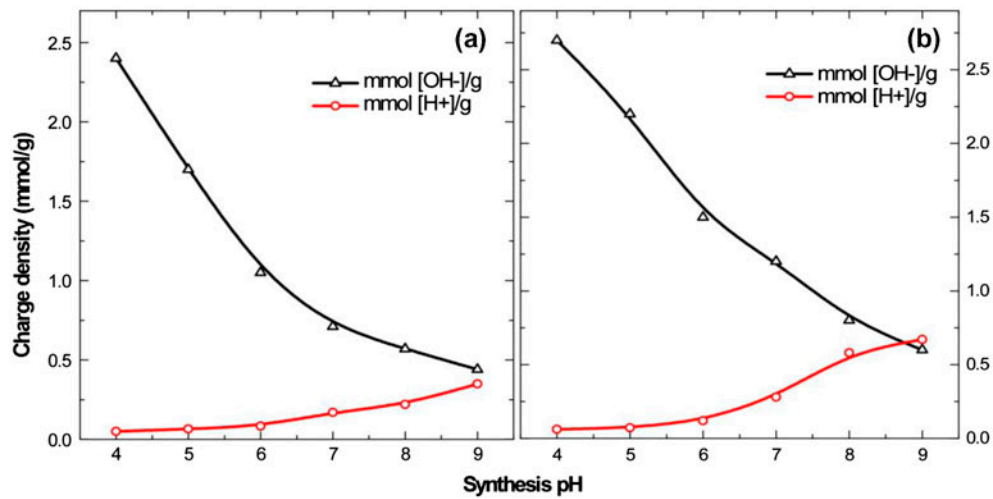


Fig. 5. Positive (mM  $[\text{OH}^-]/\text{g}$ ) and negative (mM  $[\text{H}^+]/\text{g}$ ) charge density of FeOOH (a) and FeMnOOH (b) as a function of synthesis pH.

manganese into the trivalent iron structure (Fig. 5(b)). But synthesis pH also defines the SSA which is a very important parameter in mercury uptake (Fig. 6) since it is related to the number of available adsorption sites. According to this, the higher adsorption capacity of FeMnOOH samples is mostly attributed to their significantly higher SSA values compared to the FeOOH ones. Such difference is explained by the more intense

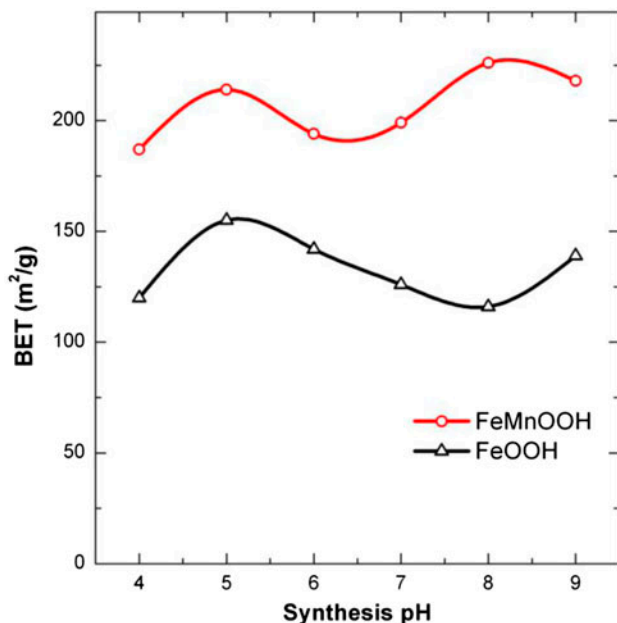


Fig. 6. SSA ( $\text{m}^2/\text{g}$ ) of FeOOH and FeMn(O)OH as a function of synthesis pH.

reaction conditions during  $\text{FeSO}_4$  precipitation by  $\text{KMnO}_4$  that favor a very rapid nucleation step and result in the production of oxyhydroxides with mean crystal size of 2 nm [30], which is lower to the respective of FeOOH [29]. The average weak increase of SSA in Fe/Mn oxyhydroxides as synthesis pH increases (from  $190 \text{ m}^2/\text{g}$  at pH 4 to  $225 \text{ m}^2/\text{g}$  at pH 9) is another explanation for the efficiency improvement presented in Fig. 3. The role of oxyhydroxides' SSA in Hg removal is also appointed for FeOOH samples by the inverse correlation of SSA values (Fig. 6) with residual concentrations (Fig. 3). For instance, the FeOOH that synthesized at pH 5 showed the higher SSA of  $155 \text{ m}^2/\text{g}$  and resulted in the lower residual concentration of  $11 \mu\text{g Hg}/\text{L}$ , while the FeOOH with the lower SSA of  $116 \text{ m}^2/\text{g}$  (synthesis pH 8) correlated with the higher residual concentration of  $15 \mu\text{g Hg}/\text{L}$ . Considering commercial iron oxyhydroxides, the efficiency of GFH and BAYOXIDE were proved significantly lower, since the residual mercury concentrations achieved were 21 and  $70 \mu\text{g}/\text{L}$  respectively.

The influence of synthesis redox in the Hg removal efficiency was studied in FeMnOOH samples prepared at the optimum pH value 6. The experimental results of Fig. 7 reveal a gradual increase of negative surface charge as the synthesis redox increases from 285 to 780 mV, which is inversely related to the residual mercury concentration. More specifically, the  $6 \mu\text{g Hg}/\text{L}$  residual concentration achieved by the samples synthesized at redox 285 mV was almost linearly decreased to around  $1 \mu\text{g}/\text{L}$  by the sample synthesized at redox 780 mV. This significant improvement in mercury uptake should be correlated only with the

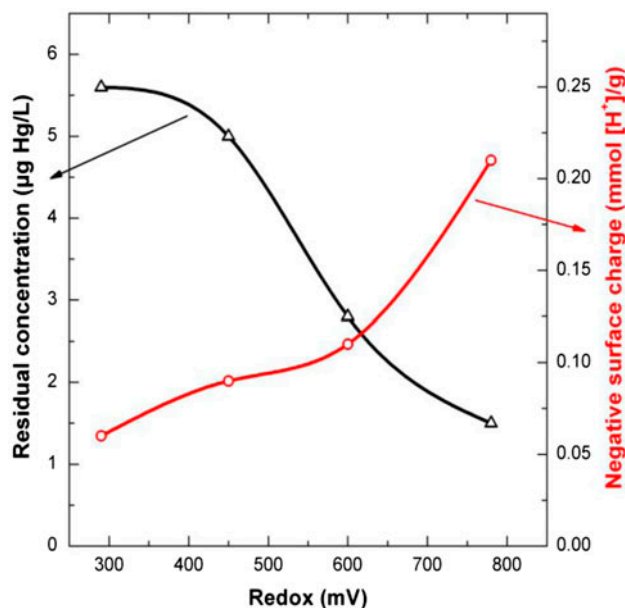


Fig. 7. Residual mercury concentration and negative surface density as a function of FeMnOOH synthesis redox. Synthesis pH 6, initial concentration 100 µg Hg/L in NSF water, adsorbent dose 100 mg/L, solution pH 7.

negative surface charge, since the SSA of samples was almost equal [30]. In addition, these results indicate the potentiality of FeMnOOH to reduce the mercury concentration down to drinking water regulation limit of 1 µg/L. Conclusively, FeMnOOH achieved significantly better mercury uptake in comparison to the FeOOH including the commercial ones. The manganese incorporation into iron oxyhydroxides provides

materials with improved SSA and negative surface charge density, with later to be significantly influenced by the synthesis pH and redox. Considering adsorbents stability the concentration of iron and manganese concentration in treated water was determined, always found below the method's detection limit of 50 and 20 µg/L, respectively.

### 3.4. Adsorption isotherms

To clarify the predominance of binary iron manganese oxyhydroxides over the single iron oxyhydroxides including the commercial ones, adsorption isotherms experiments were carried out using mercury solutions in NSF water matrix in order to get reliable and realistic information concerning the particular adsorbents' applicability. Considering the potentiality to minimize the mercury concentration down to drinking water regulation limit and using the adsorption capacity (µg Hg/mg adsorbent) as criterion, the following are concluded from Fig. 8. The commercial iron oxyhydroxides GFH and BAYOXIDE did not meet drinking water limit, since the lower residual concentration achieved was 16 and 42 µg Hg/L, respectively. In contrast, the qualified both FeOOH synthesized at pH 5 and FeMnOOH synthesized at pH 6—redox 780 mV met the first criterion by diminishing mercury concentration to regulation limit although achieving significantly different adsorption capacity. More specifically, isotherms adsorption data were best fitted both by Langmuir's and Freundlich's and the fitting parameters are presented to Table 1. This should be attributed to low equilibrium

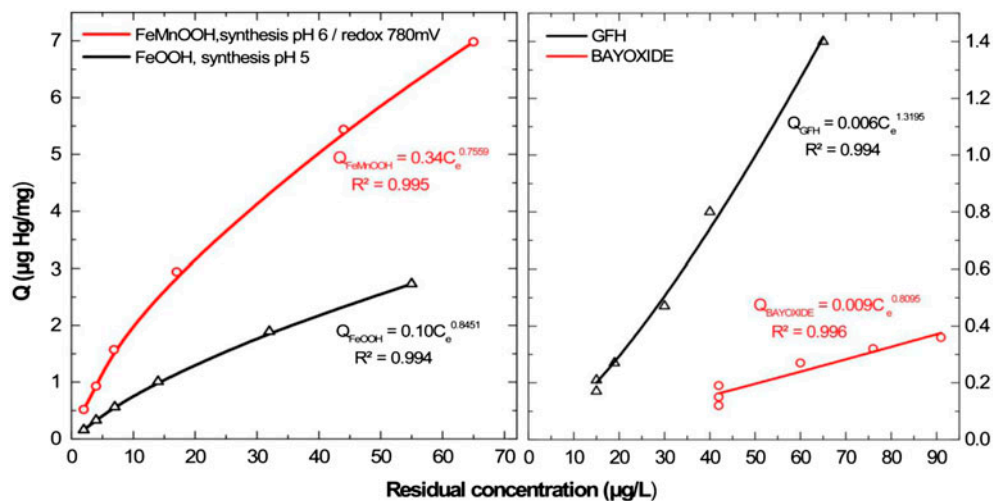


Fig. 8. Adsorption isotherms of the qualified FeOOH and FeMnOOH (a), and the commercial GFH and BAYOXIDE (b) in NSF water matrix, fitted with Freundlich's model. Note the different scale.

Table 1  
Estimated fitting parameters for Freundlich and Langmuir models

Adsorbent	$Q_1$ ( $\mu\text{g Hg}/\text{mg}_{\text{ads}}$ )	Freundlich			Langmuir		
		$K_F$ ( $\mu\text{g Hg}/\text{mg}_{\text{ads}}/(\mu\text{g}/\text{L})^{1/n}$ )	$1/\eta$	$R^2$	$K_L$ ( $\text{L}/\mu\text{g Hg}$ )	$Q_{\text{max}}$ ( $\mu\text{g Hg}/\text{mg}_{\text{ads}}$ )	$R^2$
FeMnOOH	0.34	0.34	0.756	0.995	0.022	11.9	0.998
FeOOH	0.10	0.10	0.845	0.994	0.014	6.4	0.994
GFH	–	0.006	1.319	0.994	0.006	2.2	0.958
BAYOXIDE	–	0.009	0.809	0.996	0.004	1.4	0.967

concentrations (2–80  $\mu\text{g}/\text{L}$ ) practiced, which obviously implies low surface coverage obeying to both adsorption models. The Freundlich equation is:

$$Q = K_F C_e^{1/n} \quad (2)$$

where  $Q$  is the amount of arsenic adsorbed per mass of adsorbent,  $C_e$  the equilibrium arsenic concentration,  $K_F$  and  $n$  constants related to adsorption capacity and intensity, respectively. The Langmuir equation is:

$$Q_e = \frac{Q_{\text{max}} K_L C_e}{1 + K_L C_e} \quad (3)$$

where  $Q_e$  is the quantity of arsenic adsorbed at equilibrium concentration  $C_e$ ,  $Q_{\text{max}}$  is the maximum arsenic adsorption capacity and  $K_L$  is the Langmuir constant.

After that, the adsorbents were evaluated according to the uptake capacity which corresponds to a residual mercury concentration equal to drinking water MCL of  $1 \mu\text{g}/\text{L}$ . This index, mentioned as  $Q_1$ , derives by setting  $C_e = 1 \mu\text{g}/\text{L}$  in the Freundlich equation describing each experimental isotherm. The  $Q_1$  for the binary iron manganese oxyhydroxide synthesized at pH 6 and redox 780 mV was found  $0.34 \mu\text{g Hg}/\text{mg}$  adsorbent, which counts more than 3 times of the corresponding  $0.1 \mu\text{g Hg}/\text{mg}$  adsorbent of the iron oxyhydroxide synthesized at pH 5. In addition, both commercial iron oxyhydroxides failed to meet MCL for drinking water. Conclusively, the preliminary experiments of Figs. 3 and 6 considering the improvement of FeMnOOH efficiency were verified by the adsorption isotherms data, which also indicate that binary iron manganese oxyhydroxides are promising materials for mercury removal from drinking water.

#### 4. Conclusions

Binary iron manganese oxyhydroxides were proved to be promising adsorbents for mercury removal at

residual concentrations meeting the MCL for drinking water. Synthesis parameters such as pH and redox significantly influence the adsorption efficiency for mercury of the binary iron manganese oxyhydroxides, through the SSA and negative surface charge density, although the latter showed almost no influence on the efficiency of single iron ones. A  $Q_1$ -index of  $0.34 \mu\text{g Hg}/\text{mg}$  adsorbent was determined for the qualified binary oxyhydroxide synthesized at pH 6 and redox 780 mV, while the corresponding for the single iron oxyhydroxide synthesized at pH 5 found  $0.10 \mu\text{g Hg}/\text{mg}$  adsorbent. Adsorption rapidly proceeded with 90% of the mercury to be adsorbed within 1 h. Conclusively, the FeMnOOH proved an efficient adsorbent for mercury removal at concentrations meeting drinking water regulation limits, while the commercial iron oxyhydroxides GFH and BAYOXIDE failed.

#### Acknowledgments

Program EPAN-II (OPC-II)/ESPA (NSRF): “SYNERGASIA II”, Project (MERCAP)—“Advanced Materials for Mercury Capture” (11SYN-8-206), co-Financed by the European Union and the Greek State is gratefully appreciated.

#### References

- [1] S. Mitra, Mercury in the Ecosystem, Trans Tech Publications Ltd, Aedermannsdorf, 1986.
- [2] J.W. Moore, S. Ramamoorthy, Heavy Metals in Natural Waters: Applied, Monitoring and Impact Assessment, Springer-Verlag, New York, NY, 1984.
- [3] World Health Organization, Guidelines for Drinking-water Quality, World Health Organization, Geneva, 2006.
- [4] A.J. Jacobs, S. Johnson, Groundwater and Mercury: Chemical Behavior and Treatment, Water Encyclopedia, John Wiley & Sons, Hoboken, NJ, 2005.
- [5] N. Pirrone, S. Cinnirella, X. Feng, B.R. Finkelmann, R.H. Friedli, J. Leaner, R. Mason, B.A. Mukherjee, G. Stracher, G.D. Streets, K. Telmer, Global mercury emissions to the atmosphere from natural and anthropogenic sources, in: N. Pirrone, R. Mason (Eds.), Mercury Fate and Transport in the Global Atmosphere, Springer-Verlag, New York, NY, 2009, pp. 3–49.

- [6] World Health Organization, Mercury—Environmental Aspects. Environmental Health Criteria 86, World Health Organization, Geneva, 1989.
- [7] A. Hutchison, D. Atwood, Q.E. Santilliann-Jiminez, The removal of mercury from water by open chain ligands containing multiple sulfurs, *J. Hazard. Mater.* 156 (2008) 458–465.
- [8] Y.K. Henneberry, T.E.C. Kraus, J.A. Fleck, D. Krabbenhoft, P.M. Bachand, W.R. Horwath, Removal of inorganic mercury and methylmercury from surface waters following coagulation of dissolved organic matter with metal-based salts, *Sci. Total Environ.* 409 (2011) 631–637.
- [9] US Environmental Protection Agency (EPA), Aqueous Mercury Treatment, EPA-625-R-97-004, USEPA, Cincinnati, OH, 1997.
- [10] A. Dąbrowski, Z. Hubicki, P. Podkościelny, E. Robens, Selective removal of the heavy metal ions from waters and industrial wastewaters by ion-exchange method, *Chemosphere* 56 (2004) 91–106.
- [11] V.A. Anagnostopoulos, I.D. Manariotis, H.K. Karapanagioti, C.V. Chrysikopoulos, Removal of mercury from aqueous solutions by malt spent rootlets, *Chem. Eng. J.* 213 (2012) 135–141.
- [12] L. Carro, V. Anagnostopoulos, P. Lodeiro, J.L. Barriada, R. Herrero, M.E. Sastre de Vicente, A dynamic proof of mercury elimination from solution through a combined sorption–reduction process, *Bioresour. Technol.* 101 (2010) 8969–8974.
- [13] D. Karunasagar, M.V. Balarama Krishna, S.V. Rao, J. Arunachalam, Removal and preconcentration of inorganic and methyl mercury from aqueous media using a sorbent prepared from the plant *Coriandrum sativum*, *J. Hazard. Mater.* 118 (2005) 133–139.
- [14] L. Shun-Xinga, Z. Feng-Yinga, H. Yanga, N. Jian-Conga, Thorough removal of inorganic and organic mercury from aqueous solutions by adsorption on *Lemna minor* powder, *J. Hazard. Mater.* 186 (2011) 423–429.
- [15] F. Dinatale, A. Lancia, A. Molino, M. Dinatale, D. Karatza, D. Musmarra, Capture of mercury ions by natural and industrial materials, *J. Hazard. Mater.* 132 (2006) 220–225.
- [16] M. Otero, C.B. Lopes, J. Coimbra, T.R. Ferreira, C.M. Silva, Z. Lin, J. Rocha, E. Pereira, A.C. Duarte, Priority pollutants ( $\text{Hg}^{2+}$  and  $\text{Cd}^{2+}$ ) removal from water by ETS-4 titanosilicate, *Desalination* 249 (2009) 742–747.
- [17] K.P. Lisha, S.M. Maliyekkal, T. Pradeep, Manganese dioxide nanowhiskers: A potential adsorbent for the removal of Hg(II) from water, *Chem. Eng. J.* 160 (2010) 432–439.
- [18] P.S. Mishra, S.S. Dubey, D. Tiwari, Inorganic particulates in removal of heavy metal toxic ions IX. Rapid and efficient removal of Hg(II) by hydrous manganese and tin oxides, *J. Colloid Interface Sci.* 279 (2004) 61–67.
- [19] O. Hakami, Y. Zhang, C.J. Banks, Thiol-functionalised mesoporous silica-coated magnetite nanoparticles for high efficiency removal and recovery of Hg from water, *Water Res.* 46 (2012) 3913–3922.
- [20] H. Parham, B. Zargar, R. Shiralipour, Fast and efficient removal of mercury from water samples using magnetic iron oxide nanoparticles modified with 2-mercaptobenzothiazole, *J. Hazard. Mater.* 205–206 (2012) 94–100.
- [21] M.J. Manos, V.G. Petkov, M.G. Kanatzidis,  $\text{H}_{2x}\text{Mn}_x\text{Sn}_{3-x}\text{S}_6$  ( $x=0.11\text{--}0.25$ ): A novel reusable sorbent for highly specific mercury capture under extreme pH conditions, *Adv. Funct. Mater.* 19 (2009) 1087–1092.
- [22] E.K. Faulconer, N.V.H. von Reitzenstein, D.W. Mazyck, Optimization of magnetic powdered activated carbon for aqueous Hg(II) removal and magnetic recovery, *J. Hazard. Mater.* 199–200 (2012) 9–14.
- [23] M.F. Yardim, T. Budinova, E. Ekinici, N. Petrov, M. Razvigorova, V. Minkova, Removal of mercury(II) from aqueous solution by activated carbon obtained from furfural, *Chemosphere* 52 (2003) 835–841.
- [24] G. Zelmanov, R. Semiat, Selenium removal from water and its recovery using iron ( $\text{Fe}^{3+}$ ) oxide/hydroxide-based nanoparticles sol (NanoFe) as an adsorbent, *Sep. Purif. Technol.* 103 (2013) 167–172.
- [25] E.A. Deliyanni, E.N. Peleka, K.A. Matis, Removal of zinc ion from water by sorption onto iron-based nano-adsorbent, *J. Hazard. Mater.* 141 (2007) 176–184.
- [26] I.A. Katsoyiannis, A. Zouboulis, Removal of arsenic from contaminated water sources by sorption onto iron-oxide-coated polymeric materials, *Water Res.* 36 (2002) 5141–5155.
- [27] C.R. Collins, D.M. Sherman, K.V. Ragnarsdottir, Surface complexation of  $\text{Hg}^{2+}$  on goethite: Mechanism from EXAFS spectroscopy and density functional calculations, *J. Colloid Interface Sci.* 219 (1999) 345–350.
- [28] L. Gunneriusson, S. Sjöberg, Surface complexation in the  $\text{H}^+$ -goethite ( $\alpha\text{-FeOOH}$ )-Hg (II)-chloride system, *J. Colloid Interface Sci.* 156 (1993) 121–128.
- [29] S. Tresintsi, K. Simeonidis, G. Vourlias, G. Stavropoulos, M. Mitrakas, Kilogram-scale synthesis of iron oxyhydroxides with improved arsenic removal capacity: Study of Fe(II) oxidation–precipitation parameters, *Water Res.* 46 (2012) 5255–5267.
- [30] S. Tresintsi, K. Simeonidis, S. Estradé, C. Martinez-Boubeta, G. Vourlias, F. Pinakidou, M. Katsikini, E.C. Paloura, G. Stavropoulos, M. Mitrakas, Tetravalent manganese ferrioxhyte: A novel nanoadsorbent equally selective for As(III) and As(V) removal from drinking water, *Environ. Sci. Technol.* 47 (2013) 9699–9705.
- [31] M. Kosmulski, *Surface Charging and Points of Zero Charge*, CRC Press, Boca Raton, FL, 2009.
- [32] L. Sigg, W. Stumm, The interaction of anions and weak acids with the hydrous goethite ( $\alpha\text{-FeOOH}$ ) surface, *Colloids Surf.* 2 (1980) 101–117.
- [33] C. Kim, J. Rytuba, G. Brown, EXAFS study of mercury (II) sorption to Fe- and Al-(hydr)oxides, *J. Colloid Interface Sci.* 271 (2004) 1–15.
- [34] E. Forbes, A. Posner, J. Quirk, The specific adsorption of inorganic Hg(II) species and Co(III) complex ions on goethite, *J. Colloid Interface Sci.* 49 (1974) 403–409.
- [35] Y.S. Ho, Review of second-order models for adsorption systems, *J. Hazard. Mater.* 136 (2006) 681–689.